Modelling the Energy Performance of Off-Grid Sustainable Green Cellular Base Stations

Godlove Suila Kuaban
IITiS PAN
Gliwice, Poland
gskuaban@iitis.pl

Erol Gelenbe
IITiS PAN
Gliwice, Poland &
Université Côte d'Azur, CNRS I3S
06000 Nice, France
seg@iitis.pl

Tadeusz Czachórski
IITiS PAN
Gliwice, Poland
tadek@iitis.pl

Piotr Czekalski
Silesian University of Technology
Gliwice, Poland
piotr.czekalski@polsl.pl

***Abstract*—There is a growing awareness of the need to reduce carbon emissions from the operation of mobile networks. The massive deployment of ultra-dense 5G and IoT networks will significantly increase energy demand and put the electricity grid under stress while also driving up operational costs. In this paper, we model the energy performance of an off-grid sustainable green cellular base station site which consists of a solar power system, Battery Energy Storage (BESS) and Hydrogen Energy Storage (HESS) system, and various types of macrocells, microcells, picocells, or femtocells, with broadband optical or microwave transmission systems, and other electrical and electronic systems (air conditioner, power converters, and controllers. We propose diffusion-based models of the charging and discharging processes of the energy storage systems, and obtain the probability of charging them to their full capacities during the day and completely discharging them at the end of each day. We also investigate the impact of design parameters such as the mean charging rate and the mean discharging rate on the probability densities of charging BESS and HESS to their full capacities during the day and of completely discharging them before the end of each night period.**

***Index Terms*—Diffusion process, Energy Performance, sustainability, green energy, cellular base stations, battery energy storage systems (BESS), hydrogen energy storage systems (HESS).**

I. Introduction

The exponential demand for data causes mobile network operators to constantly seek ways to increase network capacity while keeping investment and operating costs at acceptable levels. With the growing awareness about the need to reduce carbon emissions of mobile networks [1], [2], network operators put efforts to increase network capacity while minimizing energy consumption, cost and security [3]. Likewise, the European Union and other agencies have invested in many research projects in this area [4]. The massive deployment of ultra-dense 5G and IoT networks also significantly increases energy demand and drives up the network operating costs. Thus, renewable energy sources may supply small cell networks in the 5G infrastructure and IoT infrastructure, in an attempt to reduce energy costs and increase environmental sustainability [5], [6].

The authors gratefully acknowledge the partial support for this research by the European Commission's H2020 Program through the H2020 IoTAC Research and Innovation Action, under Grant Agreement No. 952684.

Mobile communications have contributed enormously to the social and economic development of every society worldwide, including the less developed or the remote parts of the world [7]. Despite the huge growth and potential of the mobile communication industry in developing countries (especially those in the Sub-Saharan African region), there re major challenges in powering existing networks (both in on-grid and off-grid areas) because of unreliable power supplies and heavy reliance on expensive diesel generators [8]. Electricity supply in sub-Saharan Africa is subject to frequent outages due to insufficient energy generation and poor transmission distribution infrastructure [9]. Also, many rural communities in these regions aren not yet connected to the grid. Thus, Information and Communication (ICT) infrastructures (e.g., base stations, network access points, transmission systems) deployed in off-grid environments can be reliably powered using energy harvesting and storage infrastructures.

There is increasing use of renewable energy to power base station sites to reduce carbon footprint and operational expenditures (OPEX) [10]. With the recent increase in energy prices, energy cost has become the dominating operational cost for mobile network operators [11]. Although the base stations of next-generation mobile networks (e.g., 5G/6G mobile networks) are designed to be energy efficient, the dense and large-scale deployment of these base stations will increase the energy demands of mobile networks. Therefore, increasing the energy mix of mobile networks to include renewable energy sources and energy storage systems could reduce the carbon emission and operation of mobile networks.

A major drawback of relying on renewable energy to directly supply base station sites is its intermittent nature, resulting in erratic and unpredictable energy production patterns [12], [13]. Energy storage systems (mostly rechargeable batteries) are often used to store excess energy, which will be used to supply the site when the renewable energy sources are unable to generate sufficient energy to meet the energy needs of the site, e.g. during the night in the case of solar plants. Deploying green energy infrastructure (e.g., photovoltaic panels and energy storage systems) requires significant Capital Expenditure (CAPEX). However, lower Operational Expenditure (OPEX) compensates for it in the medium term,

as less expensive fossil fuel energy sources are used [13].

In most off-grid renewable-based station sites, diesel generators are still used as backup energy sources to supply the site in case there is a failure in the renewable energy system (energy generation and storage systems) to generate a sufficient amount of energy to supply the site or when there is a technical failure. Diesel generators are becoming less suitable as a backup power supply system for base station sites because of challenges such as reliability, availability, high operational and maintenance costs, and negative environmental impact [14] and the limited shelf life of diesel fuel. The seasonal variation of renewable energy sources has motivated long-term energy storage systems like hydrogen to store energy during seasons with favourable weather conditions for certain renewable energy sources [14]. For example, solar energy can be harvested during spring and summer to be used during winter when there is minimal solar radiation to generate sufficient energy. Therefore, The battery is used for short-term storage to compensate for the intermittent nature of renewable sources. The hydrogen energy storage system can replace the diesel backup.

The interplay of multiple factors influencing energy generation and consumption implies that deterministic models are insufficient for the energy modelling and dimensioning off-grid green sustainable based station sites. In [15], [16] discrete energy, computation and communication units in continuous time within a Markovian framework are introduced to represent the "energy packet model" for ICT energy consumption, and various stochastic models have been applied to model the changes in the energy content of the battery energy storage of base stations [10], [12], [17], [18]. In [7] an energy packet model is developed to analyse battery storage systems to store energy in green base station sites supplied by renewable energy sources.

Recent Markovian models of energy storage systems (ESS) are based on the quantisation of energy as energy packets [19]–[24]. With data about the number of energy units delivered to the ESS within a given time interval, the mean number of energy units delivered to the ESS can be obtained, and stochastic models are then used to model the changes in the energy content of the ESS [25], [26]. One of the limitations of Markovian models is the assumption that the time required to deliver a unit of energy to the ESS is exponentially distributed, which may deviate from reality. Thus continuous state-space modelling methods such as fluid approximations, and the diffusion approximation for energy harvesting introduced in [27], were used to model the changes in the energy content of ESSs, and to estimate their relevant performance metrics [28]–[30].

A. Main contribution of the present paper

Most of the work that models solar-powered based stations the sites, does not model the day and night periods separately. The authors in [12] modelled a solar-powered base station site considering a time step granularity of 24 hours.

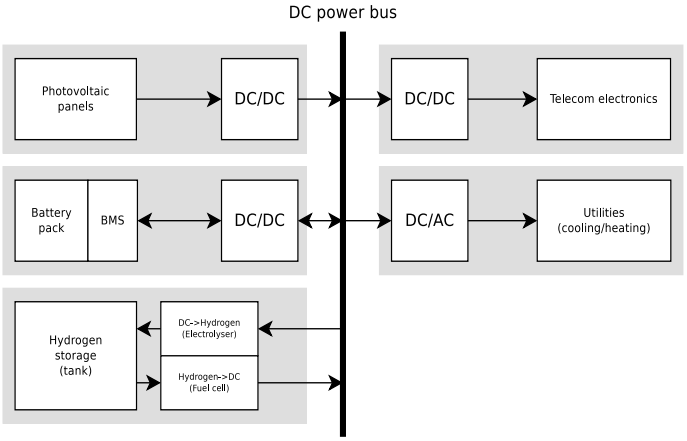

Fig. 1. A simple structure of an off-grid sustainable green base station site.

In this paper, we also model a green sustainable base station site using a time step granularity of 24 hours, but the charging process of the energy storage system comprised of a Battery Energy Storage System (BESS) and Hydrogen Energy Storage System (HESS) during the day, and the discharging process during the night, are explicitly reresented. We obtain the distribution of the energy content of BESS and HESS during the day and night, and derive the probability of charging BESS to its full capacity so that the energy harvested when BESS is full is then stored in HESS for backup or long-term storage. Thus it can be used during the worst season when insufficient energy is harvested to meet the energy demand of the base station site.

We aderive the probability of completely discharging the BESS or HESS during the night before the charging process starts, and also investigate the influence of mean charging and discharging rates on the probability of charging the ESSs to their full capacity and the probability of completely discharging them during the night.

II. The Energy Storage Systems BESS and HESS

The system we consider consits of a Base Station, PV Plant, Battery Energy Storage System (BESS), and Hydrogen Energy Storage System (HESS), as shown in Fig. 1. It is modeled over successive day and night periods of constant duration T_d and T_n; $T_d + T_n = 24$ hours.

During the day, the solar radiation is strong enough to continuously generate sufficient energy to satisfy the demand of the base station and store any excess in the battery energy storage system (BESS). If the BESS is full, the energy harvested is stored in HESS. During the night, energy is not produced, and BESS supplies the base station, and after it is completely depleted, the base station site is supplied by HESS. When HESS is empty, the entire base station site is shut down, degrading the performance of the cellular network and inflicting financial losses on the network operator.

Our model is based on diffusion approximation, a method introduced in [31]–[34] to evaluate computer systems. Here, dynamic changes in the energy content of BESS and HESS are

represented by two interacting diffusion processes. The unrestricted diffusion process has the probability density function:

$$\frac{\partial f(x,t;x_0)}{\partial t} = \frac{\alpha}{2}\frac{\partial^2 f(x,t;x_0)}{\partial x^2} - \beta\frac{\partial f(x,t;x_0)}{\partial x}, \quad (1)$$

where β and α refer to the mean and variation of the process, and x_0 is its initial value. During the day, we model the charging process by a diffusion process limited by absorbing barriers at $x = B_1$ (in the case of BESS) and $x = B_2$ (in the case of HESS), respectively; when the process comes to such a barrier, it stays there; the equation (1) is supplemented by a condition for the barrier at $x = B$

$$\lim_{x\to B} f(x,t;x_0) = 0. \quad (2)$$

Diffusion processes with one absorbing barrier was studied, in [35] and, if a process starts at $x = 0$ and ends at the barrier at $x = x_0$, ($\beta > 0$), the solution is given by Eq. (3)

$$f(x,t;0) = \frac{1}{\sqrt{2\Pi\alpha t}}\left[\exp(-\frac{(x-\beta t)^2}{2\alpha t}) - \exp(\frac{2\beta x_0}{\alpha} - \frac{(x-2x_0-\beta t)^2}{2\alpha t})\right]. \quad (3)$$

In case when the barrier is at $x = B$, and the initial condition is given by a function $\psi(\xi)$ defined on the interval $\xi \in [0.B)$ the solution for $\beta > 0$, corresponding to battery charging, becomes

$$f(x,t;\psi(\xi)) = \int_0^B f(x-\xi,t;0)\psi(\xi)d\xi. \quad (4)$$

The density of the first passage time of a diffusion process that starts from the point $x = 0$ and ends at $x = x_0$ is

$$\gamma_{0\to x_0}(t) = \lim_{x\to x_0}[\frac{\alpha}{2}\frac{\partial^2 f(x,t;0)}{\partial x^2} - \beta\frac{\partial f(x,t;0)}{\partial x}] = \frac{x_0}{\sqrt{2\Pi\alpha t^3}}e^{-\frac{(x_0-\beta t)^2}{2\alpha t}}. \quad (5)$$

Therefore, in our case, the density of the first passage time of a diffusion process that starts from the point $x = \xi$ given by a density function $\psi(\xi)$ and is absorbed at the barrier at $x = B$ is

$$\gamma_{\psi\to B}(t) = \int_0^B \frac{B-\xi}{\sqrt{2\Pi\alpha t^3}}e^{-\frac{(B-\xi-\beta t)^2}{2\alpha t}}\psi(\xi)d\xi. \quad (6)$$

Similarly, if a process starts at $x = x_0$ and ends at the barrier at $x = 0$, (with $\beta < 0$, corresponding to discharging), the solution is given by Eq. (7)

$$f(x,t;x_0) = \frac{e^{\frac{\beta}{\alpha}(x-x_0)-\frac{\beta^2}{2\alpha}t}}{\sqrt{2\pi\alpha t}}\left[e^{-\frac{(x-x_0)^2}{2\alpha t}} - e^{-\frac{(x+x_0)^2}{2\alpha t}}\right]. \quad (7)$$

In the case when the initial condition is given by a function $\psi(\xi)$ given on the interval $\xi \in [0.B)$ the solution becomes

$$f(x,t;\psi(\xi)) = \int_0^B f(x,t;\xi)\psi(\xi)d\xi. \quad (8)$$

The density of the first passage time of a diffusion process that starts from the point $x = x_0$ and ends at $x = 0$ is

$$\gamma_{x_0\to 0}(t) = \lim_{x\to 0}[\frac{\alpha}{2}\frac{\partial^2 f(x,t;x_0)}{\partial x^2} - \beta\frac{\partial f(x,t;x_0)}{\partial x}] = \frac{x_0}{\sqrt{2\Pi\alpha t^3}}e^{-\frac{(x_0+\beta t)^2}{2\alpha t}}. \quad (9)$$

The density of the first passage time of a diffusion process that starts from the point $x = \xi$ (for $\xi \in [0, \ B]$) given by a density function $\psi(\xi)$ and is absorbed at the barrier at $x = 0$ is

$$\gamma_{\psi\to 0}(t) = \int_0^B \frac{\xi}{\sqrt{2\Pi\alpha t^3}}e^{-\frac{(\xi+\beta t)^2}{2\alpha t}}\psi(\xi)d\xi. \quad (10)$$

The charging process is modelled by the diffusion process in equations (3) and (4), while the discharging process is modelled by the diffusion process in equations (7) and (8). Equation (6) represents the probability density of the charging times, and equation (10) represents the probability density of the discharging times.

During the day, the PV Plant produces energy. We see this process in a discrete way: the quanta (packets) of energy are produced and the time to produce one is random with mean $1/\lambda'$, and variance $\sigma_A^{'2}$. That means that the number of energy quanta produced during a unit of time has the normal distribution with mean λ' and variance $\lambda^{'3}\sigma_A^{'2}$.

The base station consumes a quantum of energy by the time having a distribution with mean $1/\mu$ and variance σ_B^2. We assume that during the day production is greater than consumption, and the rest of the energy is transferred to the battery BESS. The mean number of the energy packets transferred to BESS in a time unit has normal distribution is $\lambda = \lambda' - \mu$, and the variance of the number is given by $\lambda^3\sigma_A^2 = \lambda^{'3}\sigma_A^{'2} + \mu^3\sigma_B^2$. We will also use squared variation coefficients $C_A^2 = \sigma_A^2\lambda^2$, $C_B^2 = \sigma_B^2\mu^2$.

BESS has the effective capacity B_1; when it is fully charged, the energy quanta are stored in HESS having effective capacity B_2. When both BESS and HESS are full, the rest of the energy surplus is lost. At night, first the BESS feeds the base station and when it is completely discharged, HESS takes its role. When HESS becomes empty, the Base Station site is shut down.

Let us represent the energy stored in BESS and HESS by two diffusion process $X_1(t)$ on the interval $[0, B_1]$ and $X_2(t)$ on $[0, B_2]$. The intervals are limited by absorbing barriers; the process ends when it touches a barrier.

The interactions between the processes are expressed by the intensities with which they enter the barriers. During a day, $X_2(t)$ starts its movement with the intensity with which $X_1(t)$ enters the barrier at B_1. At night, $X_2(t)$ starts with the same intensity as $X_1(t)$ ends in the barrier at $x = 0$.

The process depends on its initial conditions. Except for the first cycle, these conditions are determined by the state of the processes at the end of the previous period. Therefore, we consider the processes in consecutive cycles, each composed of day and night, until their behaviour stabilises.

Let us introduce the following notation:
$f_1^{d(i+1)}(x,t;f_1^{n(i)}(x,T_n))$ is the density of $X_1(t)$ during day at cycle $(i+1)$; similarily $f_1^{n(i+1)}(x,t;f_1^{d(i)}(x,T_d))$, is its density during night, and
$f_2^{d(i+1)}(x,t;f_2^{d(i)}(x,T_n))$, $f_2^{n(i+1)}(x,t;f_2^{n(i)}(x,T_d))$ refere to the process $X_2(t)$ during day and night.

During a day, both processes have parameters $\beta_d = \lambda - \mu$, $\alpha_d = \lambda^3\sigma_A^2 + \mu^3\sigma_B^2$ and during night $\beta_n = -\mu$, $\alpha_n = \mu^3\sigma_B^2$.

Consider the day period number $i+1$. During it, first BESS is filled. The density of the process is defined by Eqs. (3), (4):

$$f_1^{d(i+1)}(x,t;f_1^{n(i)}(x,T_n)) \quad = \\ = \int_0^{B_1} \frac{1}{\sqrt{2\Pi\alpha_d t}}\left[\exp(-\frac{(x-\xi-\beta_d t)^2}{2\alpha_d t}) \right. \\ \left. -\exp(\frac{2\beta_d B_1}{\alpha_d} - \frac{(x-\xi-2B_1-\beta_d t)^2}{2\alpha_d t})\right] f_1^{n(i)}(\xi,T_n)d\xi. \quad (11)$$

BESS is fully charged when the process attains the absorbing barrier at $x = B_1$. This time corresponds to the first passage time from points given by the initial distribution $f_1^{n(i)}(x,T_n)$ to B_1; its density is

$$\gamma^{d(i+1)}_{1,f_1^{n(i)}(x,T_n)\to B_1}(t) = \int_0^{B_1} \gamma^{d(i+1)}_{1,\xi\to B_1}(t)\, f_1^{n(i)}(\xi,T_n)d\xi. \quad (12)$$

The flow entering the barrier is accumulated there and represents the probability that BESS is full

$$p_{B_1}^{d(i+1)}(t) = \int_0^t \gamma^{d(i+1)}_{1,f_1^{n(i)}(x,T_n)\to B_1}(\tau)d\tau \quad (13)$$

The process $X_2(t)$ is initiated with the intensity $\gamma^{d(i+1)}_{1,f_1^{n(i)}(x,T_n)\to B_1}(t)$ given by Eq. (12), therefore its density at time t is composed of pdfs of all processes started at time $\tau < t$:

$$f_2^{d(i+1)}(x,t;f_2^{n(i)}(x,T_n)) \quad = \quad (14) \\ = \int_0^t f_2^{d(i+1)}(x,t-\tau;f_2^{n(i)}(x,T_n))\gamma^{d(i+1)}_{1,f_1^{n(i)}(x,T_n)\to B_1}(\tau)d\tau.$$

In a similar way, the density of the first passage time to B_2 is obtained as

$$\gamma^{d(i+1)}_{2,f_2^{n(i)}(x,T_n)\to B_2}(t) \quad = \\ = \int_0^t \int_0^{B_2} \gamma^{d(i+1)}_{2,\xi\to B_2}(t-\tau)\, f_2^{n(i)}(\xi,T_n)d\xi\gamma^{d(i+1)}_{1,f_1^{n(i)}(x,T_n)\to B_1}(\tau)d\tau \quad (15)$$

At night, first BESS is being discharged. The initial condition of the process is defined by the distribution $f_1^{d(i+1)}(x,T_d)$ at the end of the day. We compute $f_1^{n(i+1)}(x,t;f_1^{d(i+1)}(x,T_d))$ in the similar way as at day period, using Eqs. (7), (8) and taking into account the night diffusion parameters β_n, α_n (time is set to zero)

$$f_1^{n(i+1)}(x,t;f_1^{d(i)}(x,T_d)) \quad = \\ = \int_0^{B_1} \frac{e^{\frac{\beta}{\alpha}(x-\xi)-\frac{\beta^2}{2\alpha}t}}{\sqrt{2\pi\alpha t}}\left[e^{-\frac{(x-\xi)^2}{2\alpha t}} - e^{-\frac{(x+\xi)^2}{2\alpha t}}\right] f_1^{d(i)}(\xi,T_d)d\xi. \quad (16)$$

Then we determine the density of the distribution of the first passage time to $x = 0$, after which BESS is completely discharged

$$\gamma^{n(i+1)}_{1,f_1^{d(i+1)}(x,T_d)\to 0}(t) = \int_0^{B_1} \gamma^{n(i+1)}_{1,\xi\to 0}(t) f_1^{d(i+1)}(\xi,T_d)d\xi,$$

The same density is also the rate at which HESS is activated. Similarly to the day period, the pdf of the energy of HESS during the night is

$$f_2^{n(i+1)}(x,t;f_2^{d(i+1)}(x,T_d)) \quad = \quad (17) \\ = \int_0^t f_2^{n(i+1)}(x,t-\tau;f_2^{d(i+1)}(x,T_d))\, \gamma^{d(i+1)}_{1,f_1^{n(i)}(x,T_n)\to 0}(\tau)d\tau.$$

Similarly, the density of the first passage time to B_2 is obtained as

$$\gamma^{d(i+1)}_{2,f_2^{d(i)}(x,T_d)\to B_2}(t) \;=\; \int_0^t \int_0^{B_2} \gamma^{d(i+1)}_{2,\xi\to B_2}(t-\tau)\, f_2^{d(i)}(\xi,T_d)d\xi \\ \gamma^{d(i+1)}_{1,f_1^{d(i)}(x,T_d)\to B_1}(\tau)d\tau \quad (18)$$

The probabilities $p_{1,0}^{n(i+1)}(t)$, $p_{2,0}^{n(i+1)}(t)$ denote the time-dependent probabilities that BESS and HESS are empty at night

$$p_{1,0}^{n(i+1)}(t) = \int_0^t \gamma^{n(i+1)}_{1,f_1^{d(i+1)}(x,T_d)\to 0}(\tau)d\tau, \quad (19)$$

$$p_{2,0}^{n(i+1)}(t) = \int_0^t \gamma^{n(i+1)}_{2,f_2^{d(i+1)}(x,T_d)\to 0}(\tau)d\tau. \quad (20)$$

We assume any initial conditions for the first cycle ($i = 1$) and iterate to reach the point of convergence, where

$$f_1^{n(i+1)}(x,t;f_1^{d(i)}(x,T_d)) \approx f_1^{n(i)}(x,t;f_1^{d(i-1)}(x,T_d).$$

Based on these fixed point distributions, we may compute the time distribution after which BESS and HESS become empty at night, complete at day, probabilities that they are empty or full as a function of time, etc.

III. Numerical examples

We present numerical results that provide insights into the energy performance of the base station site, specifically the outage probability of the site, which is the probability that the energy stored in both the battery energy storage system and the hydrogen energy storage system is completely depleted. We assume that $B_1 = 50$ KWh and $B_2 = 50$ KWh. The initial conditions for the beginning of the first day are $x_0 = 25$ KWh for BESS and $x_0 = 0$ for HESS.

Fig. 2 illustrates the probability density of the charging process. It gives the distribution of the energy content of BESS at the end of the day in each 24-hour cycle i. It can be seen that after $i = 7$ day cycles, the probability density functions converge. The pdf for the discharging process shown in Fig. 3 equally converges after $i = 7$ day cycles.

Figs. 4 and 5 show the probability density of the energy content of BESS at the end of the day and the end of the night for $i = 20$ day cycle. The density at the end of the day is shifted to the right because, at the end of the day,

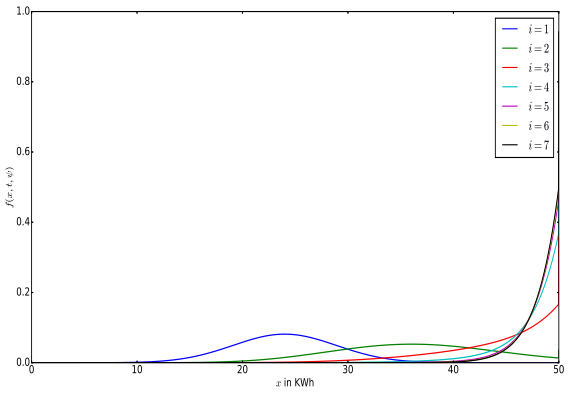

Fig. 2. The convergence of the probability densities, $f_1^{d(i)}(x, T_d, \psi)$ of the energy content of BESS at the end of each day cycle $i = 1, \ldots 7$ for $\mu = 1$ KW, $\lambda = 2$ KW, $C_A^2 = C_B^2 = 1$, $T_d = T_n = 12$ hours.

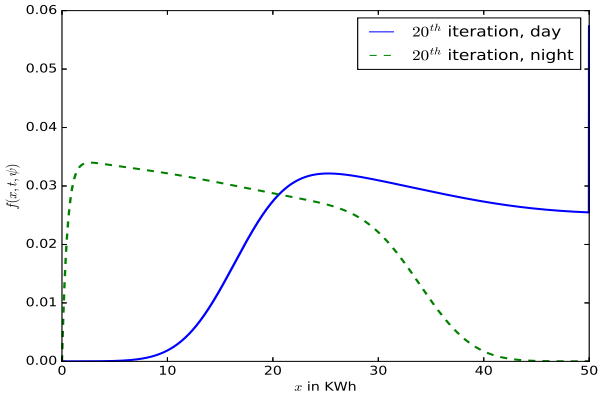

Fig. 5. The probability densities, $f_1^{d(20)}(x, T_d, \psi)$, $f_1^{n(20)}(x, T_n, \psi)$ of the energy content of BESS at the end of the day and night of $i = 20$ day cycle for $\mu = 1$ KW, $\lambda = 2$ KW, $C_A^2 = C_B^2 = 1$, $T_d = 8$ hours and $T_n = 16$ hours.

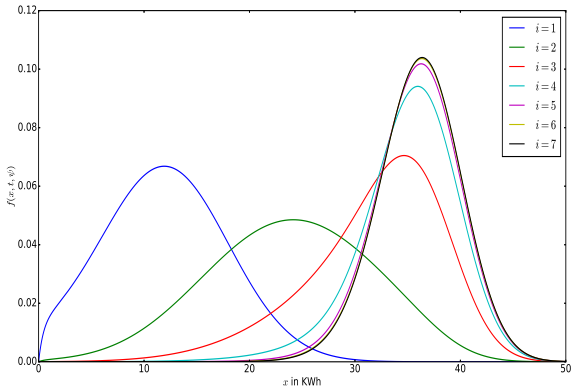

Fig. 3. The convergence of the probability densities, $f_1^{n(i)}(x, T_n, \psi)$ of the energy content of BESS at the end of each night cycle $i = 1, \ldots 7$ for $\mu = 1$ KW, $\lambda = 2$ KW, $C_A^2 = C_B^2 = 1$, $T_d = T_n = 12$ hours.

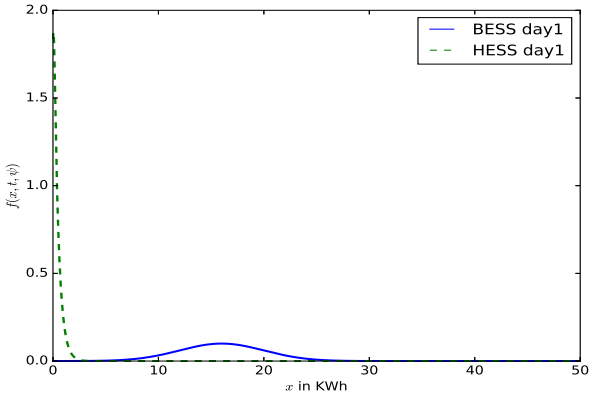

Fig. 6. The probability densities, $f_1^{d(1)}(x, T_d, \psi)$, $f_2^{d(1)}(x, T_d, \psi)$ of the energy content of BESS and HESS at the end of the day for the $i = 1$ day cycle for $\mu = 1$ $\lambda = 2$ KW, $C_A^2 = C_B^2 = 1$, $T_d = 8$ hours and $T_n = 16$ hours.

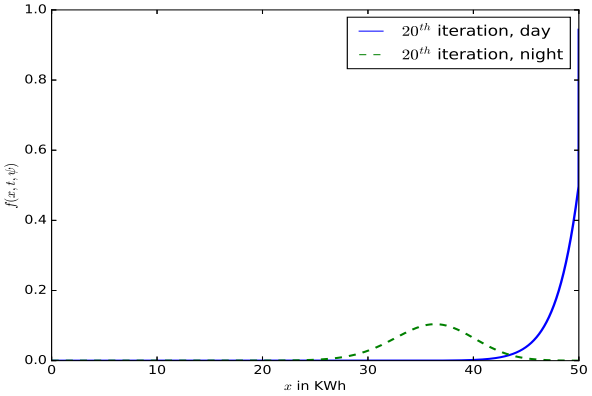

Fig. 4. The probability densities, $f_1^{d(20)}(x, T_d, \psi)$, $f_1^{n(20)}(x, T_n, \psi)$ of the energy content of BESS at the end of the day and night of $i = 20$ day cycle for $\mu = 1$ KW, $\lambda = 2$ KW, $C_A^2 = C_B^2 = 1$, $T_d = T_n = 12$ hours.

the probability that BESS is charged to its full capacity is high. In contrast, the density of the energy content of BESS at the end of the night is shifted to the left because, at night, BESS is discharged to supply the base station site, reducing its energy content. In Fig. 4, we consider that day and night hours are equal, that is, $T_d = T_n = 12$ hours. For the given site parameter configuration, the probability that BESS will be completely discharged is low. However, in Fig. 5, $T_d = 8$ hours and $T_n = 16$ hours (we have shorter days and longer nights like during winter), the probability of charging BESS to its full capacity is low and the probability that BESS will be completely discharged before the charging process begins at the start of the next day increases. In this case, the energy stored in HESS will be used as a backup if BESS is discharged entirely.

Figs. 6–10 show the probability densities of the energy content of BESS and HESS at the end of the day for the $i = 1$ day cycle. Figs. 6, 7, and 10 show the influence of the

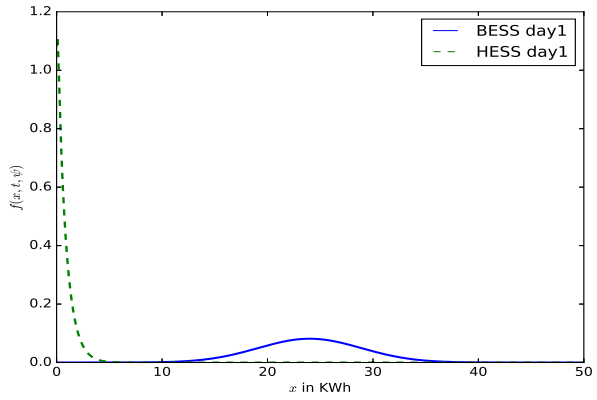

Fig. 7. The probability densities $f_1^{d(1)}(x,T_d,\psi)$, $f_2^{d(1)}(x,T_d,\psi)$ of the energy content of BESS and HESS at the end of the day for the $i=1$ day cycle for $\mu=1$ KW, $\lambda=2$ KW, $C_A^2=C_B^2=1$, $T_d=T_n=12$.

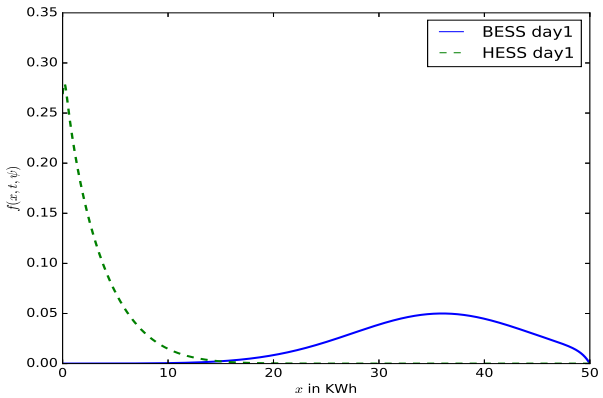

Fig. 8. The probability densities $f_1^{d(1)}(x,T_d,\psi)$, $f_2^{d(1)}(x,T_d,\psi)$ of the energy content of BESS and HESS at the end of the day for the $i=1$ day cycle for $\mu=1$ KW, $\lambda=3$ KW, $C_A^2=2$, $C_B^2=1$, $T_d=T_n=12$ hours.

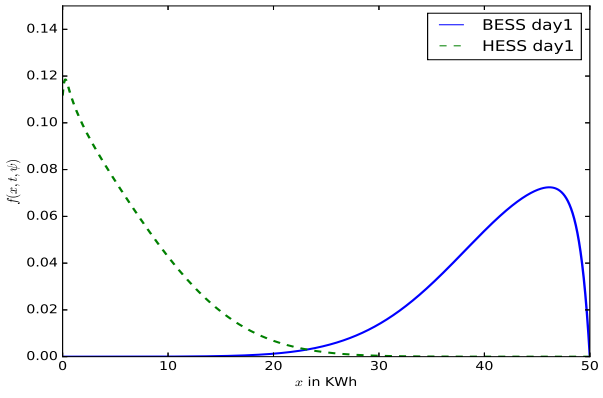

Fig. 9. The probability densities $f_1^{d(1)}(x,T_d,\psi)$, $f_2^{d(1)}(x,T_d,\psi)$ of the energy content of BESS and HESS at the end of the day for the $i=1$ day cycle for $\mu=1$ KW, $\lambda=4$ KW, $C_A^2=2$, $C_B^2=1$, $T_d=T_n=12$ hours.

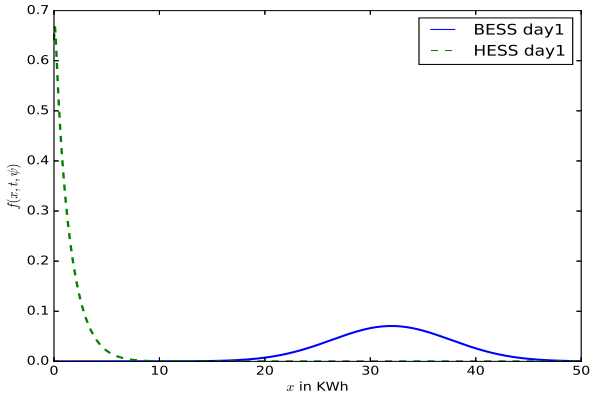

Fig. 10. The probability densities, $f_1^{d(1)}(x,T_d,\psi)$, $f_2^{d(1)}(x,T_d,\psi)$ of the energy content of BESS and HESS at the end of the day for the $i=1$ day cycle for $\mu=1$ $\lambda=2$ KW, $C_A^2=C_B^2=1$, $T_d=16$ hours and $T_n=8$ hours.

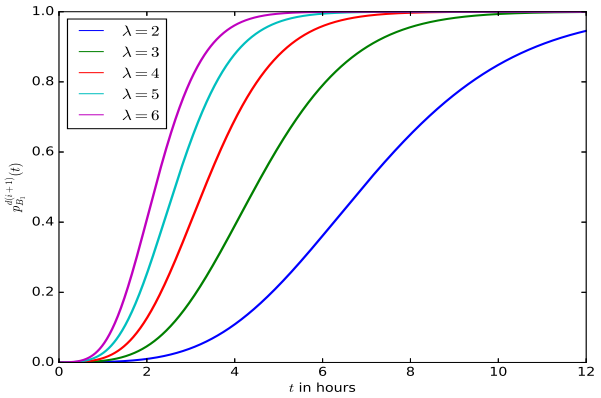

Fig. 11. The influence of mean charging rate, λ on the probability of charging BESS during the day, $p_{B_1}^{d(7)}(t)$ for, $i=7$, $\mu=1$ KW, $C_A^2=C_B^2=1$, $T_d=T_n=12$ hours.

number of hours of day and night on the probability densities of the energy content of BESS and HESS at the end of the day for $\mu=1$ $\lambda=2$ KW, $C_A^2=C_B^2=1$. It can be seen that as the number of hours of day increases, more energy is stored in BESS. When BESS is full, additional energy generated is stored in HESS (illustrated by the right shift of the densities as T_d increases). Figs 8 and 9 show the influence of the mean rate at which energy is delivered to the energy storage system (BESS and BESS), λ on the probability densities of the energy content at BESS and HESS at the end of the day for $\mu=1$ KW, $C_A^2=2$, $C_B^2=1$, $T_d=T_n=12$ hours. It can be seen that the densities for $\lambda=4$ (Fig. 9) are shifted to the right (with a higher probability of charging BESS to its full capacity and storing more energy in BESS to be used as backup or during the season when solar energy generation is poor) compared to the densities for $\lambda=3$ KW (Fig. 8).

Figs. 11 and 12 show the influence of λ on the probability of charging BESS to its full capacities during the day and of

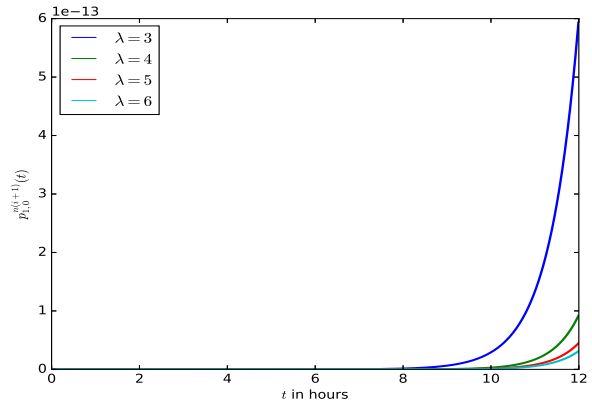

Fig. 12. The influence of mean charging rate λ on the probability of discharging BESS during the night, $p_{1,0}^{n(7)}(t)$ for, $i = 7$, $\mu = 1$ KW, $C_A^2 = C_B^2 = 1$, $T_d = T_n = 12$ hours.

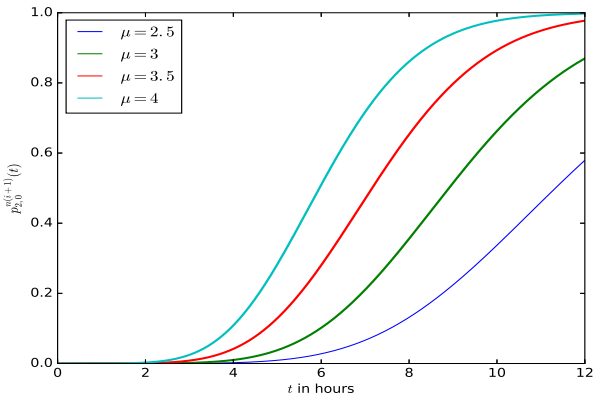

Fig. 13. The influence of mean discharging rate μ on the probability of discharging BESS during the night, $p_{1,0}^{n(7)}(t)$ for $i = 7$, $\lambda = 2$ KW, $C_A^2 = C_B^2 = 1$, $T_d = T_n = 12$ hours.

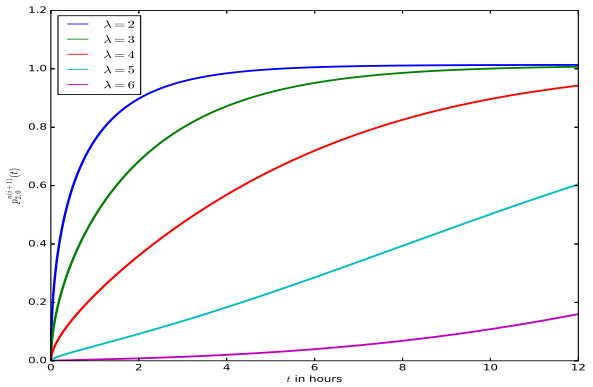

Fig. 14. The influence of mean charging rate λ on the probability of discharging HESS during the first night, $p_{2,0}^{n(1)}(t)$ for, $i = 1$ $\mu = 1$ KW, $C_A^2 = C_B^2 = 1$, $T_d = T_n = 12$ hours.

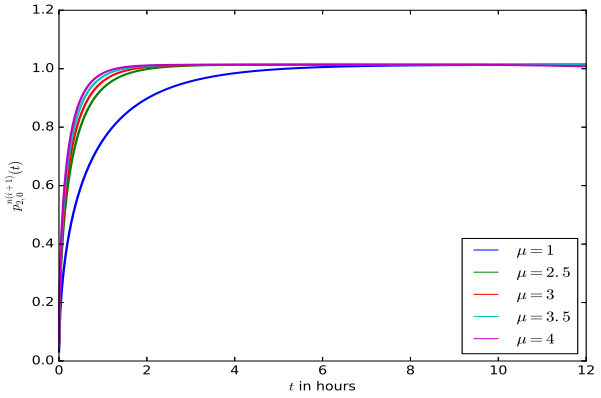

Fig. 15. The influence of mean discharging rate μ on the probability of discharging HESS during the first night, $p_{2,0}^{n(1)}(t)$ for, $i = 1$ $\lambda = 2$ KW, $C_A^2 = C_B^2 = 1$, $T_d = T_n = 12$ hours.

completely discharging it during the night, respectively, for $\mu = 1$ KW, $C_A^2 = C_B^2 = 1$, $T_d = T_n = 12$ hours. As λ increases, the probability of charging BESS to its full capacity increases and the probability that it will be discharged entirely during the night decreases.

Fig. 13 shows the influence of the energy demand of the base station site, μ, on the probability of completely discharging BESS during the night. As μ increases, the probability that BESS will be discharged entirely before the next charging cycle begins increases. Therefore, if the energy demand of the base station site increases (may be due to deploying more microcells, picocells, or femtocells on the site or due to increased demand for cooling), the energy generation capacity should also be increased proportionately.

Fig. 14 shows the influence of mean charging rate λ on the probability of discharging HESS during the night for $\mu = 1$ KW, $C_A^2 = C_B^2 = 1$, $T_d = T_n = 12$ hours. As λ increases, the probability of discharging HESS decreases because with a higher energy delivery rate to BESS, it will quickly charge to its full capacity, and more energy will be stored in HESS, decreasing the probability of discharging HESS when the energy source is absent. Fig. 15 shows the influence of mean discharging rate μ on the probability of discharging HESS during the night for, $\lambda = 2$ KW, $C_A^2 = C_B^2 = 1$, $T_d = T_n = 12$ hours. As μ increases, the probability of discharging HESS when the source is absent (at night) increases as more energy is required to supply the base station site, quickly draining BESS and drawing more energy from HESS.

The depletion probabilities are for the chosen parameters high. In subsequent cycles, the energy stored in HESS will be increased, playing the role of real backup for BESS. The volume of HESS should also be increased.

IV. Conclusions

We have modelled the energy performance of an off-grid sustainable green cellular base station which includes a solar

power plant, energy storage systems (BESS and HESS), for various types of base stations, macrocells, microcells, picocells, or femtocells, with broadband optical or microwave transmission systems, and other electrical and electronic systems (air conditioner, power converters, and controllers. A diffusion process with absorbing barriers represents the energy at each storage system. This approach enabled us to include the means and variances of energy production and consumption processes, leading to greater realsim than Markovian models. The proposed coordination of diffusion processes responsible for BESS and HESS with the diffusion first passage time density may be extended to more complex systems of batteries, and their charging and discharging patterns.

We modelled the charging and discharging processes of the energy storage systems to obtain the distribution of their energy content at every moment, particularly at the end of each day and night, and the probability of charging the BESS and HESS to their full capacities during the day and completely discharging them at the end of each night. We also investigated the impact of the design parameters' impact, such as the mean charging and discharging rates, on these probabilities. The proposed models can be applied to size the energy generation, storage, and consumption requirements for off-grid sustainable green cellular base stations.

REFERENCES

[1] L. Chang, F. Taghizadeh-Hesary, and H. B. Saydaliev, "How do ict and renewable energy impact sustainable development?" *Renewable Energy*, vol. 199, pp. 123–131, 2022. [Online]. Available: https://www.sciencedirect.com/science/article/pii/S0960148122012484

[2] M. Mohsin, F. Taghizadeh-Hesary, N. Iqbal, and H. Saydaliev, "The role of technological progress and renewable energy deployment in green economic growth," *Renewable Energy*, vol. 190, p. 777787, 2022. [Online]. Available: https://doi.org/10.1016/J.RENENE.2022.03.076

[3] O. Brun, Y. Yin, E. Gelenbe, Y. M. Kadioğlu, and J. Augusto-Gonzalez, "Deep learning with dense random neural networks for detecting attacks against IoT-connected home environments," in *Security in Computer and Information Sciences: First International ISCIS Security Workshop 2018, Euro-CYBERSEC 2018, London, UK, February 26-27, 2018, Revised Selected Papers*. Springer International Publishing, 2018, pp. 79–89.

[4] M. U. Çağlayan, "Review of some recent european cybersecurityresearch and innovation projects," *Infocommunications Journal*, no. 4, pp. 70–78, 2022.

[5] B. Pernici, M. Aiello, J. Vom Brocke, B. Donnellan, E. Gelenbe, and M. Kretsis, "What is can do for environmental sustainability: a report from caise'11 panel on green and sustainable is," *Communications of the Association for Information Systems*, vol. 30, no. 1, p. 18, 2012.

[6] A. Israr, Q. Yang, W. Li, and A. Y. Zomaya, "Renewable energy powered sustainable 5g network infrastructure: Opportunities, challenges and perspectives," *Journal of Network and Computer Applications*, vol. 175, pp. 1–24, 2021.

[7] E. Gelenbe and O. H. Abdelrahman, "An energy packet network model for mobile networks with energy harvesting," *Nonlinear Theory and Its Applications*, vol. 9, no. 3, pp. 322–322, 2018.

[8] S. Kumar, "Tower power africa: Energy challenges and opportunities for the mobile industry," *Africa. Tech*, 2014.

[9] D. Farquharson, P. Jaramillo, and C. Samaras, "Sustainability implications of electricity outages in sub-saharan africa," *Nature Sustainability*, vol. 1, pp. 589–597, 2018.

[10] H. Wang, H. Li, L. Ye, X. Chen, H. Tang, and S. Ci, "Modeling, metrics, and optimal design for solar energy-powered base station system," *Journal on Wireless Communications and Networking*, vol. 39, pp. 1–17, 2015.

[11] N. Piovesan, A. F. Gambin, M. Miozzo, and M. R. and, "Energy sustainable paradigms and methods for future mobile networks: A survey," *Computer Communications*, vol. 119, pp. 101–117, 2018.

[12] D. Renga and M. Meo, "Dimensioning renewable energy systems to power mobile networks," *IEEE Transactions on Green Communications and Networking*, vol. 3, no. 2, pp. 366–380, 2019.

[13] M. Dalmasso, M. Meo, and D. Renga, "Radio resource management for improving energy self-sufficiency of green mobile networks," *ACM SIGMETRICS Performance Evaluation Review*, vol. 44, no. 2, pp. 82–87, 2016.

[14] A. Mohamad Aris and B. Shabani, "Sustainable power supply solutions for off-grid base stations," *Energies*, vol. 8, no. 10, pp. 10 904–10 941, 2015.

[15] E. Gelenbe, "Energy packet networks: Ict based energy allocation and storage," in *International Conference on Green Communications and Networking*. Springer, 2011, pp. 186–195.

[16] ——, "Energy packet networks: Smart electricity storage to meet surges in demand," in *Proceedings of the 5th International ICST Conference on Simulation Tools and Techniques*, ser. SIMUTOOLS '12. Brussels, BEL: ICST (Institute for Computer Sciences, Social-Informatics and Telecommunications Engineering), 2012, p. 17.

[17] D. Renga and M. Meo, "Modeling renewable energy production for base stations power supply," in *2016 IEEE International Conference on Smart Grid Communications (SmartGridComm)*, 2016, pp. 716–722.

[18] C. Zeljkovic, P. Mrsic, B. Erceg, D. Lekic, N. Kitic, and P. Matic, "Optimal sizing of photovoltaic-wind-diesel-battery power supply for mobile telephony base stations," *Energy*, vol. 242, p. 122545, 2022.

[19] E. Gelenbe, "A sensor node with energy harvesting," *ACM SIGMETRICS Performance Evaluation Review*, vol. 42, no. 2, pp. 37–39, 2014.

[20] Y. M. Kadioğlu, "Finite capacity energy packet networks," *Probability in the Engineering and Informational Sciences*, vol. 31, no. 4, pp. 477–504, 2017.

[21] ——, "Energy consumption model for data processing and transmission in energy harvesting wireless sensors," in *International Symposium on Computer and Information Sciences*, 2016, pp. 117–125.

[22] Y. M. Kadioğlu and E. Gelenbe, "Product-form solution for cascade networks with intermittent energy," *IEEE Systems Journal*, vol. 13, no. 1.

[23] M. U. Çağlayan, "G-Networks and their applications to Machine Learning, Energy Packet Networks and Routing: Introduction to the Special Issue," *Probability in the Engineering and Informational Sciences*, vol. 31, no. 4, pp. 381–395, 2017.

[24] E. Gelenbe and Y. Zhang, "Performance optimization with energy packets," *IEEE Systems Journal*, vol. 13, no. 4, pp. 3770–3780, 2019.

[25] Y. Zhang, "Optimal energy distribution with energy packet networks."

[26] ——, "G-Networks and the Performance of ICT with Renewable Energy," *SN Computer Science*, vol. 1, no. 1, 2020.

[27] O. H. Abdelrahman and E. Gelenbe, "A diffusion model for energy harvesting sensor nodes," in *2016 IEEE 24th International Symposium on Modeling, Analysis and Simulation of Computer and Telecommunication Systems (MASCOTS)*. IEEE, 2016, pp. 154–158.

[28] L. X. Cai, Y. Liu, T. H. Luan, X. S. Shen, J. W. Mark, and H. V. Poor, "Sustainability analysis and resource management for wireless mesh networks with renewable energy supplies," *IEEE Journal On Selected Areas in Communications*, vol. 32, no. 2, pp. 345–355, 2014.

[29] T. Czachórski, E. Gelenbe, and G. S. Kuaban, "Modelling energy changes in the energy harvesting battery of an iot device," in *Proceedings of the 2022 30th International Symposium on Modeling, Analysis, and Simulation of Computer and Telecommunication Systems (MASCOTS)*. Nice, France: IEEE, 2022, pp. 81–88.

[30] T. Czachórski, E. Gelenbe, G. S. Kuaban, and D. Marek, "Energy optimization for an unmanned aerial vehicle (e.g drone) during its mission," in *Security in Computer and Information Sciences. EuroCybersec 2021. Communications in Computer and Information Science*, vol. 1596. Springer, 2022, pp. 61–75.

[31] H. Kobayashi, "Application of the diffusion approximation to queueing networks II: Equilibrium queue distributions," *Journal of the ACM (JACM)*, vol. 21, no. 3, pp. 316–328, 1974.

[32] ——, "Application of the diffusion approximation to queueing networks II: Non-equilibrium distributions and applications to computer modeling," *Journal of the ACM (JACM)*, vol. 21, no. 3, pp. 459–469, 1974.

[33] E. Gelenbe, "On approximate computer systems models," *Journal of the ACM*, vol. 22, no. 2, pp. 261–269, 1975.

[34] ——, "Probabilistic models of computer systems, Part II: Diffusion approximations, waiting times and batch arrivals," *Acta Informatica*, vol. 12, no. 4, pp. 285–303, 1979.

[35] R. P. Cox and H. D. Miller, *The Theory of Stochastic Processes*. London, UK: Chapman and Hall, 1965.